Estonian Journal of Engineering, 2012, **18**, 1, 58–75 doi: 10.3176/eng.2012.1.05

Exploring vibrations of cracked beams by the Haar wavelet method

Ülo Lepik

Institute of Mathematics, University of Tartu, Liivi 2, 50409 Tartu, Estonia; ulo.lepik@ut.ee

Received 9 September 2011

Abstract. Free and forced vibrations of cracked Euler–Bernoulli beams are analysed by the Haar wavelet method. Stiffness reduction for open V-shaped edge cracks is calculated. To demonstrate the efficiency of the proposed method, three problems about bending and vibration of cantilever beams are solved. The obtained results are compared with available data of other authors.

Key words: Euler–Bernoulli beams, free and forced vibrations, cracks, Haar wavelet method.

1. INTRODUCTION

Cracks, occurring in structural elements, may significantly change the behaviour of the whole structure and therefore the development of reliable crack models has been the objective of many investigations. Due to the great number of published papers we cite here only some of them, which are nearer to the topic of the present paper. More complete analysis can be found in overviews, from which we note here [1,2].

There are different possibilities for crack modelling. The conventional approach is to divide the beam-type structure into two parts that are pinned at the crack location and the crack is simulated by a massless torsional spring [3–8]. Continuity of deflection, bending moment and shear force is imposed, the slope is discontinuous at the crack section $x = \xi$ and we have

$$w'(\xi + 0) - w'(\xi - 0) = Cw''(\xi). \tag{1}$$

Here w stands for deflection of the beam, C denotes the flexibility of the spring; it is a function of the crack depth and beam height. Different formulas for its calculation are proposed [4,7–9]. This approach is a simplification of crack dynamics since the crack size and structure are not involved directly.

More exact solutions can be obtained by applying two- or three-dimensional finite element meshes. To avoid large errors in calculation, a very fine mesh is needed; this requires a large computational effort. To enlighten the computational burden, continuous crack models have been introduced. Evidently, here the first paper belongs to Christides and Barr [10] from 1984. A V-shaped crack model was proposed by Sinha et al. [11]. Approximation of this model by exponential function is given in [12], where the effect of the stress concentration in the vicinity of the cracked region was estimated by the so-called crack disturbance function.

In most papers open cracks are considered. In fact, cracks can open and close in time depending on the loading conditions and vibration amplitude (breathening cracks); such cracks were treated in [13–16]. In some cases closed form solutions for damaged beams are obtained. Making use of the theory of the generalized functions (distributions) it is possible to integrate the equations of motion analytically and in this way to get exact solutions for the cracked beams [16–21].

For analysing the beam structures with singularities, a great popularity have obtained the wavelet-based methods, since they are very accurate in detecting the localized abnormalities. First papers about this topic appeared in 90-es, an overview of them can be found in [22]. In most papers the wavelet methods were applied for the detection and identification of cracks. Here for the given signal the wavelet transforms are accomplished at different levels of resolution (scales). If the resolution is fine enough, transient vibrations become evident in some region; this allows us to detect the crack and its location. This approach was applied in several papers from which we cite here [22–26].

Among the wavelet families, special attention deserve the Haar wavelets. They are made up of pairs of piecewise constant functions and therefore are mathematically the simplest orthogonal wavelets with a compact support. They can be integrated analytically arbitrary times. A drawback of these wavelets is the fact that they are not continuous and therefore cannot be differentiated at the points of discontinuity. To overcome this difficulty, we expand into the Haar wavelet series not the function itself but its highest derivative appearing in the differential equation to be solved. The lower derivatives and the function itself are found by integration. This approach has turned out to be very successful for solving differential and integral equations [27–30].

The main aim of the present paper is to demonstrate the efficiency of the Haar wavelet method for exploring transverse vibrations of cracked Euler–Bernoulli beams. The paper is organized as follows. In Section 2 the governing equations of the problem are presented. Some versions of the crack models are discussed in Section 3. Integrals of the Haar wavelets are presented in Section 4. Bending of beams under statical loading is examined in Section 5. In Sections 6 and 7 free and forced vibrations of beams with singularities are analysed.

2. GOVERNING EQUATIONS

Consider an Euler–Bernoulli beam of rectangular cross-section, which carries a concentrated load $\tilde{F}$ at the cross-section $\tilde{x} = \tilde{x}*$. The equations of motion are

$$\frac{\partial \tilde{M}}{\partial \tilde{x}} = -\tilde{Q}, \quad \tilde{M} = -EI(\tilde{x})\frac{\partial^2 \tilde{w}}{\partial \tilde{x}^2}, \quad I(\tilde{x}) = (1/12)bh(\tilde{x})^3,$$
$$\frac{\partial \tilde{Q}}{\partial \tilde{x}} = -\mu \frac{\partial^2 \tilde{w}}{\partial t^2} + \tilde{F}\delta(\tilde{x} - \tilde{x}_*), \tag{2}$$

where $\mu = bh(\tilde{x})\rho$. Here E is the Young modulus, $I(\tilde{x})$ is the moment of inertia of the cross-section, $\tilde{M}$ and $\tilde{Q}$ denote the bending moment and shear force, respectively. The beam's length is L, dimensions of its cross-section are b and $h(\tilde{x})$, ρ denotes the density of the beam material, $\tilde{w}$ means the deflection, and $\delta(\tilde{x} - \tilde{x}_*)$ is the Dirac delta function.

In the following only motion with an harmonic load $\tilde{F} = F\exp(i\omega t)$ is considered. By introducing the symbols

$$w = \tilde{w}\exp(-i\omega t), \ M = \tilde{M}\exp(-i\omega t), \ Q = \tilde{Q}\exp(-i\omega t), \ x = \tilde{x}/L \tag{3}$$

we find (primes denote differentiation with regard to x)

$$M' = -LQ, \quad M = -EI(x)w''/L^2, \quad Q' = \mu L\omega^2 w + F\delta(x - x_*). \tag{4}$$

Equations (4) can be rewritten in the form

$$(G(x)w'')'' = A\gamma\omega^2 w + BF\delta(x - x_*). \tag{5}$$

Here the following symbols are introduced

$$\gamma(x) = h(x)/h(0), \quad G(x) = \gamma(x)^3, \quad h_0 = h(0), \tag{6}$$

$$A = \frac{12\rho L^4}{E{h_0}^2}, \quad B = \frac{12}{Eb}\left(\frac{L}{h_0}\right)^3. \tag{7}$$

Integrating (5) twice, we find

$$Gw'' = \Omega\int_0^x dx\int_0^x \gamma w dx = BF(x - x_*)U(x - x_*) + C_1 x + C_2. \tag{8}$$

Here $\Omega = A\omega^2$ and U denotes the Heaviside function ($U = 0$ for $x < x_*$ and $U = 1$ for $x \geq x_*$). The integration constants C_1 and C_2 are calculated from the boundary conditions for M and Q. In the following only the case of a cantilever beam, for which $M(1) = Q(1) = 0$, is considered. Besides, it is assumed that the load F acts in the end section $x = 1$. For this case the integro-differential equation (8) obtains the form

$$Gw'' - \Omega\left[-\int_x^1 dx\int_0^x \gamma w dx + (1 - x)\int_0^1 \gamma w dx\right] = BF(1 - x). \tag{9}$$

3. MODELLING CRACKS

There are different ways for crack modelling. In this Section three of them are considered. To demonstrate the benefits and shortcomings of these models the following simple problem is solved. We consider pure static bending of a cantilever beam, which has a crack at $x = \xi$. The crack has uniform depth d across the width of the beam and is fully open. The relative depth of the crack is $\beta = d/h$. In view of (4) we have

$$G(x)W'' = 2, \quad \text{where} \quad W = -2EI(0)w/(ML^2). \tag{10}$$

Here the symbol $G(x)$ denotes the non-dimensional flexural rigidity of the beam. For Eq. (10) closed form solutions can be found.

3.1. First model [21]

According to the conventional approach (1) we assume that the crack is concentrated in a single section of the beam and assume

$$G(x) = 1 - \Gamma\delta(x - \xi). \tag{11}$$

In this section it is assumed that the cracks are modelled as notches (saw-cuts). In such a case the parameter Γ is related with the relative depth of the crack β by the formula

$$\Gamma = 1 - G(\xi) = 1 - (1 - \beta)^3. \tag{12}$$

Replacing (11) into (10), we obtain

$$[1 - \Gamma\delta(x - \xi)]W'' = 2. \tag{13}$$

Making use of the algebra of distributions, this result can be put into the form [17]

$$W'' = 2\left[1 + \frac{\Gamma}{1 - \alpha\Gamma}\delta(x - \xi)\right]. \tag{14}$$

Here for evaluating the product of the two deltas, the following formula was applied [17]:

$$\delta(x - \xi)\delta(x - \xi) = \alpha\delta(x - \xi), \quad \alpha = 2.013. \tag{15}$$

By integrating this equation twice we find (the symbol U denotes the Heaviside function)

$$\begin{aligned} W' &= 2\left[(x + \frac{\Gamma}{1 - \alpha\Gamma}U(x - \xi)\right], \\ W &= x^2 + \frac{2\Gamma}{1 - \alpha\Gamma}(x - \xi)U(x - \xi). \end{aligned} \tag{16}$$

This model has an essential shortcoming. According to (14), the inequality $1 - \alpha\Gamma > 0$ holds, consequently $\Gamma < 1/\alpha$ and $\beta < 0.205$. So we see that this model is applicable only for modelling cracks of small depth. It is shown in [21] that Eqs (16) are equivalent with the results obtained for the beam model with an internal torsional spring.

3.2. The second model

Cerri and Vestroni [31] proposed a crack model with constant stiffness reduction due to a crack. This case can be realized if we present Γ by two Heaviside functions:

$$G = 1 - \Gamma U(x - \xi + \lambda) + \Gamma U(x - \xi - \lambda). \tag{17}$$

Here λ denotes the non-dimensional effective width of the crack. Making again use of the algebra of distributions, we can put (17) into the form

$$W'' = 2 + \frac{2\Gamma}{1-\Gamma}[U(x - \xi + \lambda) - U(x - \xi - \lambda)], \tag{18}$$

from which follows

$$W = x^2 + \frac{\Gamma}{1-\Gamma}\left[(x - \xi + \lambda)^2 U(x - \xi + \lambda) - (x - \xi - \lambda)^2 U(x - \xi - \lambda)\right]. \tag{19}$$

3.3. The third model

V-shaped cracks were considered in [10]. In this case we have

$$G(x) = \left\{ \begin{array}{lll} 1 - (\Gamma/\lambda)(x - \xi + \lambda) & \text{for} & \xi - \lambda < x \le \xi, \\ 1 + (\Gamma/\lambda)(x - \xi - \lambda) & \text{for} & \xi < x \le x + \xi, \\ 1 \quad elsewhere. & & \end{array} \right\}. \tag{20}$$

Since analytic integration of (13) is somewhat troublesome, we have carried out this operation numerically. For the Models II–III the parameter λ, determining the effective width in the cracked zone, must be known. In the case of saw-cut type cracks it is prescribed. As to fatigue cracks, here different formulas are proposed. Most of them can be written in the form

$$\lambda = K(\beta)h_0/L. \tag{21}$$

According to Christides and Barr [10], a good approximation gives $K(\beta) = 1.5$. Bilello [32] recommended to take $K(\beta) = \beta/0.9$. A more complicated formula belongs to Bovsunovsky and Matveev [14], which has the form

$$K(\beta) = \frac{0.3675(1-\beta)}{1-(1-\beta)^3}[(1-\beta)^6 - 3(1-\beta)2 + 2]. \tag{22}$$

The calculation of λ can be avoided if we approximate (20) by an expression involving an exponential function [11]:

$$G(x) = \frac{1-\Gamma}{1-\Gamma+\Gamma\exp[-2\alpha|x-\xi|L/h]}. \qquad (23)$$

The value $\alpha = 0.667$ is estimated from experimental data.

Computer simulation was carried out for ξ = 0.5 and L/h = 20. Slopes and deflections versus coordinate x for the first two models and for β = 0.15 are plotted in Figs 1 and 2. Besides the deflections at the beam end, $WF = W(1)$ were calculated. The results for all the three models were WF_I = 2.73, WF_{II} = 1.010, WF_{III} = 1.005. For β= 0.5 we found WF_{II} = 1.117, WF_{III} = 1.117 (the first model is not applicable).

For a V-shaped crack, deflections at the beam end $x = 1$ were calculated for alternative values of the parameter λ. The results are presented in Table 1.

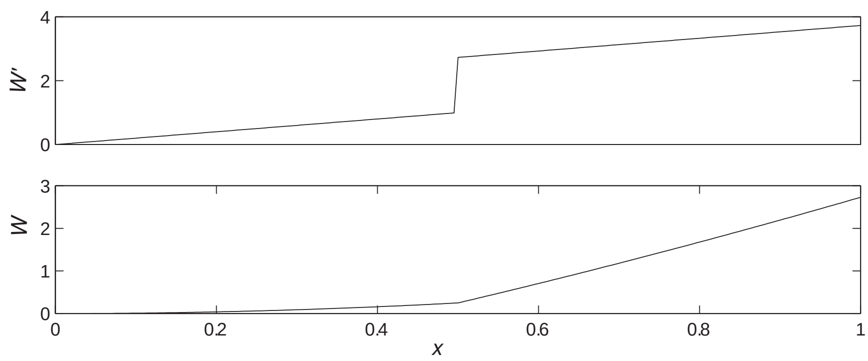

Fig. 1. Slope and deflection of the cracked beam (model I).

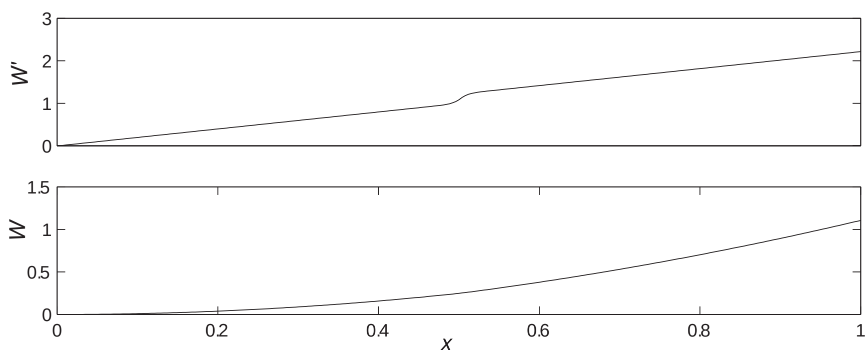

Fig. 2. Slope and deflection of the cracked beam (model II).

Table 1. Deflections at the beam end for different values of L/h and β

L/h	β	W_1	W_2	W_3	W_4
20	0.25	1.013	1.024	1.011	1.103
	0.40	1.042	1.143	1.025	1.272
	0.50	1.074	1.206	1.033	1.525
50	0.25	1.006	1.037	1.005	1.051
	0.40	1.020	1.071	1.011	1.136
	0.50	1.025	1.102	1.014	1.262

Here for calculating W_1, the formula $K = \beta/0.9$ was applied, in the case of W_2 if was assumed $K = 1.5$. For calculating W_3 and W_4, the formulas (22) and (23) were used, respectively.

It follows from Table 1 that the gap between these solutions may be quite significant. Unfortunately it is not possible to apply for λ a universal criterion since the reliability of one or other criterion depends upon the character of the problem to be solved. Therefore, making use of the available experimental data or carrying out some test calculations with the aid of a more exact method (e.g., by FEM) the validity of one or another method should be cleared out, after that the main part of computations are carried out by the wavelet method. This approach demands some complementary work, but this is compensated by the simplicity of the Haar wavelet solutions.

4. THE HAAR WAVELET METHOD

Let us consider the interval $x \in [A, B]$, where A and B are given constants. We shall define the quantity $M = 2^J$, where J is the maximal level of resolution. The interval $[A, B]$ is divided into $2M$ subintervals of equal length; the length of each subinterval is $\Delta x = (B-A)/(2M)$. Next, two parameters are introduced: the dilatation parameter $j = 0, 1, ..., J$ and the translation parameter $k = 0, 1, ..., m-1$ (here the notation $m = 2^j$ is introduced). The wavelet number i is defined as $i = m + k + 1$. The i-th Haar wavelet is defined as (Fig. 3)

$$h_i(x) = \begin{cases} 1 & \text{for } x \in [\xi_1(i), \xi_2(i)]\,, \\ -1 & \text{for } x \in [\xi_2(i), \xi_3(i)]\,, \\ 0 & \text{elsewhere}\,, \end{cases} \tag{24}$$

where

$$\begin{aligned} \xi_1(i) &= A + 2k\mu\Delta x\,, & \xi_2(i) &= A + (2k+1)\mu\Delta x\,, \\ \xi_3(i) &= A + 2(k+1)\mu\Delta x\,, & \mu &= M/m\,. \end{aligned} \tag{25}$$

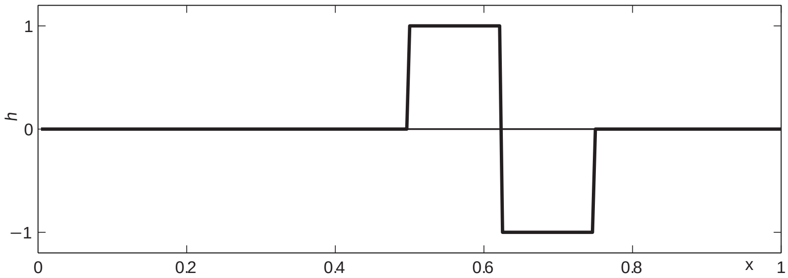

Fig. 3. Haar wavelet for $J = 2, \quad i = 7.$

The case $i = 1$ corresponds to the scaling function $h_1(x) = 1$ for $x \in [A, B]$, and $h_1(x) = 0$ elsewhere.

If we want to solve a n-th order ODE, we need the integrals

$$p_{\nu,i}(x) = \underbrace{\int_A^x \int_A^x \dots \int_A^x}_{\nu-\text{times}} h_i(t)dt^\nu = \frac{1}{(\nu-1)!} \int_A^x (x-t)^{\nu-1} h_i(t)dt, \tag{26}$$

$$\nu = 1, 2, ..., n\,, \quad i = 1, 2, ..., 2M.$$

The case $\nu = 0$ corresponds to the function $h_i(t)$. Taking account of [28−30], these integrals can be calculated analytically; by doing it we obtain

$$p_{\alpha,i}(x) = \left\{ \begin{array}{l} 0 \\ \qquad\qquad \text{for } \ x < \xi_1(i)\,, \\ \frac{1}{\alpha!}[x - \xi_1(i)]^\alpha \\ \qquad\qquad \text{for } \ x \in [\xi_1(i), \xi_2(i)]\,, \\ \frac{1}{\alpha!}\left\{[x - \xi_1(i)]^\alpha - 2[x - \xi_2(i)]^\alpha\right\} \\ \qquad\qquad \text{for } \ x \in [\xi_2(i), \xi_3(i)]\,, \\ \frac{1}{\alpha!}\left\{[x - \xi_1(i)]^\alpha - 2[x - \xi_2(i)]^\alpha + [x - \xi_3(i)]^\alpha]\right\} \\ \qquad\qquad \text{for } \ x > \xi_3(i)\,. \end{array} \right\}. \tag{27}$$

These formulas hold for $i > 1$. In the case $i = 1$ we have $\xi_1 = A, \ \xi_2 = \xi_3 = B$ and

$$p_{\alpha,1}(x) = \frac{1}{\alpha!}(x - A)^\alpha\,. \tag{28}$$

In this paper the governing equation (9) is solved by the collocation method.

The collocation points are (the symbol $x(l)$ denotes the grid points)

$$x_c(l) = 0.5[x(l-1) + x(l)], \quad l = 1, 2...2M. \tag{29}$$

Let us introduce the vector of the wavelet coefficients $a = (a_i), i = 1, 2, \dots, 2M$ and define the Haar matrices

$$H(i,l) = h_i[x_c(l)], \quad P_\alpha(i,l) = p_{\alpha,i}[x_c(l)], \\ i,l = 1,2,...2M, \quad \alpha = 1,2,3... . \tag{30}$$

Solution of Eq. (9) is sought in the matrix form $w'' = aH$. By integrating this equation and taking into account the boundary conditions, we find

$$w' = aP_1, \quad w = aP_2. \tag{31}$$

Next we introduce notations

$$I_{1i}(x) = \int_0^x \gamma(x) p_{2i}(x) dx, \quad I_{2i}(x) = \int_0^x dx \int_0^x \gamma(x) p_{2i}(x) dx. \tag{32}$$

These results are introduced into Eq. (9); the outcome can be put into the matrix form as

$$aR = BF(E - x_c), \tag{33}$$

where

$$R(i,l) = G(l)H(i,l) + \Omega[E(l) - x_c(l)]I_{1i}(1) - I_{2i}(1) + I_{2i}[x_c(l)], \\ i,l = 1,2,...,2M. \tag{34}$$

Here E is a $2M$ unit vector. The wavelet coefficients a_i are calculated by solving the system (33), the slope and deflection are computed from Eq. (31).

To demonstrate the efficiency of the proposed method, in the following sections three problems are solved.

5. BENDING OF MULTI-CRACKED BEAMS

In the paper [8] by Skrinar the following problem was solved by the finite element method. A cantilever beam of length L = 8 m and height h= 0.18 m carries a concentrated load F = 10 kN at the beam's end. The Young's modulus is E = 30 GPa. At the distances 1, 4 and 6 m, three cracks are present. The depths of all cracks were taken to be 0.09 m.

Let us solve this problem by the Haar wavelet method. We start from Eqs (33)–(34) by assuming Ω = 0. In the present case B = 0.3512. The dimensionless crack locations and depths are ξ_1= 0.125, ξ_2 = 0.50, ξ_3 = 0.75, β_1 = β_2 = β_3 = 0.5. V-shaped cracks are assumed. The function $G(x)$ is calculated according to Eq. (20). For the level of resolution, the value $J = 7$ was taken. Computer simulation was carried out for $\lambda = (\beta/0.9)(h/L)$ and for $\lambda = 1.5h/L$. Deflection at the beam end was found to be 12.71 and 15.40, respectively (Skrinar got the value 14.42). To improve these solutions, we demand that the angle at the crack tip should be the

Table 2. Deflections of the beam end (in cm)

	First crack	Second crack	Third crack	Under the force
Skrinar	0.263	4.483	9.097	14.417
Wavelet	0.219	4.430	8.980	14.223

same for the functions $\gamma = \gamma(x)$ and $G = G(x)$. If we denote by Λ the effective crack width for $G = G(x)$, then $\lambda/\beta = \Lambda/\Gamma$ and $\Lambda = \Gamma\lambda/\beta = \Gamma h/(0.9L)$.

We have replaced in Eq. (20) $\lambda \to \Lambda$ and executed the calculations once more. The results are presented in Table 2.

It follows from Table 2 that the accordance of both solutions may be regarded as satisfactory. The Skrinar's computation model consisted of 14,400 2D eight noded finite elements and about 90,000 linear equations were solved. Our method is much simpler, since for $J = 7$ only 256 equations had to be solved.

6. FREE VIBRATIONS OF BEAMS WITH SINGULARITIES

In the case of free vibrations we take $F = 0$ in Eq. (33). This system is now linear and has non-trivial solutions only if the determinant is 0. This requirement is fulfilled only for some discrete values of $\Omega = \Omega_\nu,\ \nu = 1, 2, 3...$ The eigenfrequencies of the beam are $\omega_\nu = \sqrt{\Omega_\nu/A}$, where the coefficient A is calculated from Eq. (7). If we want to obtain the deflection modes then we must fix the deflection at some point, assuming, e.g., $w(1) = 1$ and adding this requirement to the system (33). The augmented system is non-homogeneous and can be solved in the ordinary way. If cracks appear, the non-dimensional rigidity in the damaged zone is calculated according to Eq. (20). Following Eq. (11), we assume that cracks do not change the beam mass; consequently, they do not have an effect in calculation of the integrals $I_{1i}(x)$ and $I_{2i}(x)$; this circumstance greatly simplifies the solution. Essential is the choice of the parameter λ, which determines the extent of the cracked zone. Our computations have shown that the Bilello criterion gives for eigenfrequencies mostly overestimated, and the Christides–Barr criterion – underestimated values. By this reason we have made use of the estimate $\lambda = \Gamma h/(0.9L)$, which was discussed in Section 5; since $\beta \leq \Gamma \leq 1$, this criterion gives for λ intermediate values to be compared with the other two criteria.

At first, vibrations of a uniform beam with a single crack at $x = \xi$ is considered. Since $\gamma(x) \equiv 1$, evaluation of the integrals (34) gives $I_{1i}(x) = p_{3i}(x)$, $I_{2i}(x) = p_{4i}(x)$. Equation (33) obtains the form

$$R(i, l) = G(l)H(i, l) + \Omega\{[1 - x_c(l)]p_{3,i}(1) - p_{4,i}(1) + P_4(i, l)\}. \qquad (35)$$

To start, the uncracked beam is considered. Carrying out computations for $J = 6$, we found $\Omega_1^{(0)} = 12.3627, \Omega_2^{(0)} = 485.48$; the exact values are exactly the same. It follows that the accuracy of the wavelet solution is very high already for the level $J = 6$.

Free vibrations of a cantilever beam with a crack location $x = 0.275$ were considered by Sinha et al. [11]. The relative crack depths β were 0.16, 0.32 and 0.48. The solution was obtained by using a FEM model with rotational springs (16 elements with 34 degrees of freedom). Numerical results were checked with the experimental data. Let us compare these data with our wavelet results. The reduction of the frequency of vibrations due to the cracks is estimated by the coefficient

$$\Delta_\nu = \sqrt{\Omega_\nu / \Omega_\nu^{(0)}}, \quad \nu = 1, 2, \ldots . \tag{36}$$

Results of computation are shown in Table 3. The symbols Δ_{theor} and Δ_{exp} indicate the theoretical and experimental values taken from Table 2 of the paper [11], Δ_{wav} corresponds to the wavelet solution. Analysis of these data shows that in comparison with the experiment our solution is not worse than the Sinha's FEM solution.

Free vibrations of a two-stepped beam with two cracks, supposed to belong to different steps, were analysed by Zhang et al. [23]. The cracks were modelled by springs, the cracks and the step divided the beam into four sub-beams; the governing equations were solved by the method of transfer matrix. In the following the solution, based on the Haar wavelet method, is presented. Let us assume that the step is located at $x = \eta$, the locations of the cracks are ξ_1 and ξ_2, and their depths are β_1 and β_2. The non-dimensional height of the beam $\gamma(x)$ is now specified and we can evaluate the integrals (32). By doing this we find

$$\begin{gathered} I_{1i}(1) = \gamma_1 p_{3i}(1) - (1 - \gamma_1) p_{3,i}(\eta), \\ I_{2i}(x_l) = P_4(i,l) + \{-(1-\gamma_1)[P_i(i,l) - p_{4,i}(\eta) - p_{3,i}(\eta)(x_l - \eta)]\} U(x_l - \eta), \end{gathered} \tag{37}$$

where U is the Heaviside function. The cracks are modelled according to Eq. (20). The effective width of cracks is taken again in the form $\Lambda = \Gamma h/(0.9L)$; in the case of a stepped beam, the parameter Γ is calculated from the formula $\Gamma = \gamma^3 - (\gamma - \beta)^3$. Computer simulation was carried out for the Cases 3 and 8 of the paper [23]. The results are shown in Figs 4 and 5 and in Table 4. In Table 4, the

Table 3. Reduction of eigenfrequencies of cracked beams, comparison of the results with [11]

	Mode 1			Mode 2		
β	Δ_{theor}	Δ_{exp}	Δ_{wav}	Δ_{theor}	Δ_{exp}	Δ_{wav}
0.16	0.987	1.000	0.995	0.997	0.998	0.992
0.32	0.974	0.969	0.980	0.993	0.997	0.997
0.48	0.962	0.950	0.956	0.990	0.991	0.994

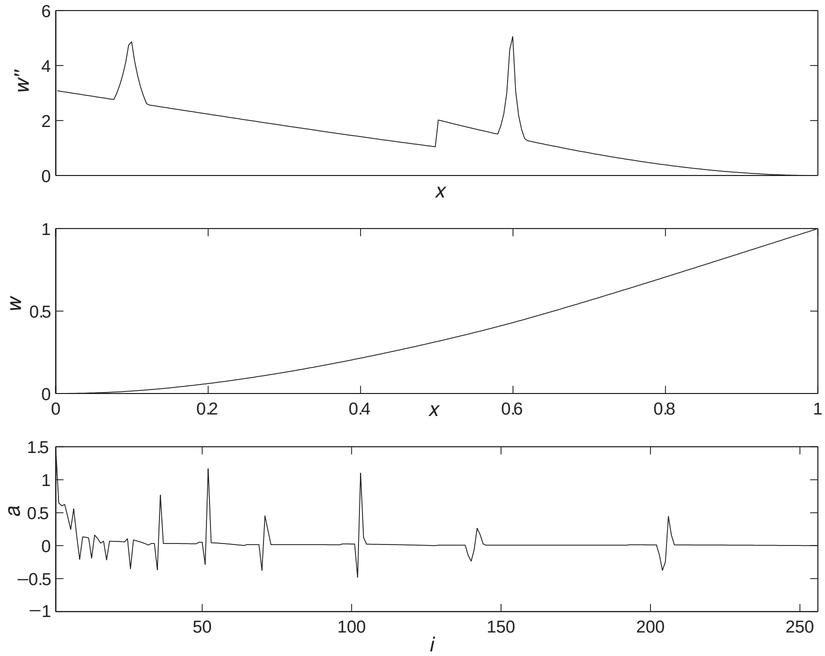

Fig. 4. Curvature, deflection and wavelet coefficients for Problem 3 from [23]; first mode.

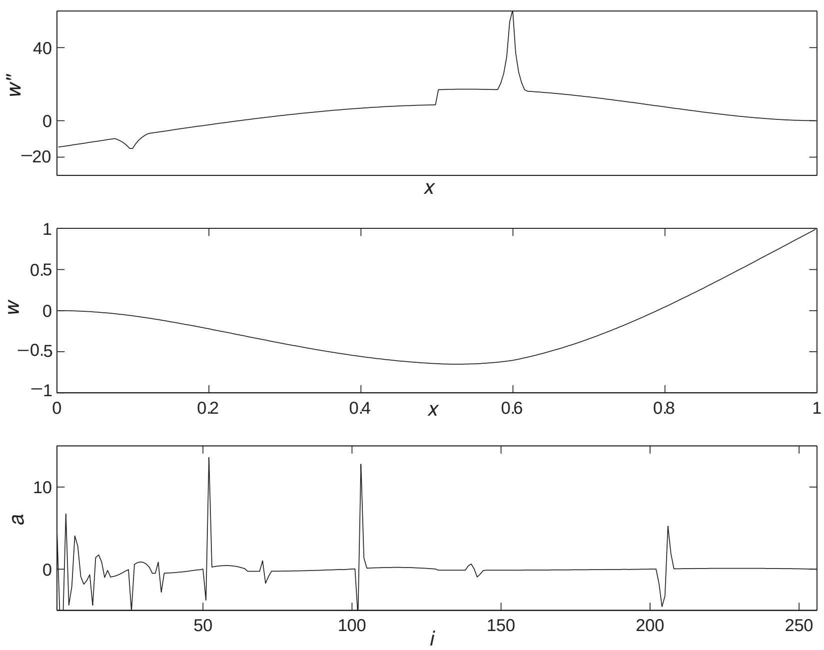

Fig. 5. Curvature, deflection and wavelet coefficients for Problem 3 from [23]; second mode.

Table 4. Reduction of eigenfrequencies of cracked beams, comparison of the results with [23]

	Case 3		Case 8	
Mode	Δ_{Zh}	Δ_{wav}	Δ_{Zh}	Δ_{wav}
1	0.977	0.977	0.947	0.949
2	0.985	0.984	0.948	0.964

symbols Δ_{Zh} correspond to the solutions of paper [23], the symbols Δ_{wav} to our wavelet solution. It follows from Table 4 that the accordance of these solutions is very good for the first mode and somewhat worse in the case of the second mode. With reference to Figs 4 and 5 we would like to turn attention to the fact that most of the wavelet coefficients are zero; this is typical to the discrete wavelet methods and to a great extent increases the speed of convergence.

The wavelet method is very convenient for treating stepped beams. According to the conventional approach, the beam is divided into sub-beams between the steps; governing equations are solved for each beam separately, satisfying the continuity equations at each step. This procedure may turn to be very troublesome, especially if the number of steps is more than two. The wavelet solution is much more simple, since the beam is treated as a whole (not divided into sub-beams).

7. FORCED VIBRATIONS OF THE BEAM

Vibrations of cracked cantilever beams under a concentrated harmonic load were discussed by Orhan et al. [9]. Single and double V-shaped cracks were considered. For solution, the ANSYS 8.0 program was used, the beam was discretized into 1520 elements with 2300 nodes. The beam and material parameters were $L = 0.5\,\text{m}$, $b = 0.2\,\text{m}$, $h = 0.029\,\text{m}$, $E = 206.8\,\text{GPa}$, $\rho = 7780\,\text{kg/m}^3$. Now let us solve the same problem by the wavelet method. For this again Eq. (5) must be solved. The values of the coefficients in Eq. (7) are A = 3.420e-6, B = 1.487e-5. Computer simulation was carried for two cases from [11]: 1) a single crack at ξ_1 = 0.75, 2) two cracks at ξ_1 = 0.5, ξ_2 = 0.75. In both cases for the cracks depths d the values 8, 20 and 24 mm were taken. The forcing frequency $f_r = \omega/(2\pi)$ is prescribed, the natural frequency is calculated as $f_n = (1/(2\pi L)\sqrt{\Omega/A}$. In the case of the uncracked beam we have f_0 = 605.18 (this is an exact value); the wavelet solution for J = 7 gives 605.19, which practically coincides with the exact value. In the case of damaged beams the crack model (20) is applied for $\lambda = \Gamma h/(0.9L$. The matrix $R(i, l)$ can be calculated according to Eq. (35), taking into account the formula $\Omega = A\omega^2$. The wavelet coefficients (a_i) are calculated by solving the system (33). Slope and deflection are evaluated from Eq. (31).

First, let us calculate the end deflection $W =\mid w(1) \mid$ as a function of the forcing frequency f_r. The result for undamaged beam is plotted in Fig. 6. It

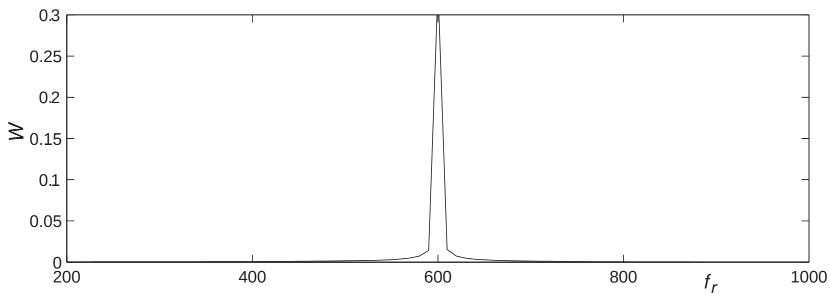

Fig. 6. Maximal deflection of the uncracked beam versus forcing frequency.

can be seen that here from a background of low intensity arises a sharp peak. This is evidently the phenomenon of resonance. In the case of cracked beams the resonance frequencies decrease. This a quite different result to be compared with the paper [[9]], where the curves $W = W(f_r)$ had a broad specter and no sharp resonance peaks appeared. Our solution seems to be logical, since no viscosity is taken into account. In [[9]], the FEM was applied; perhaps by that some artificial or hidden viscosity was introduced and due to it the signal was smeared out to some region.

As to cracked beams, by increasing the cracks depth the resonance frequency decreases. This effect is quite small in the case of single cracks (the same conclusion is made in [[9]]).In the case of two cracks, the computer simulation gave (in parentheses are the values of the dominant peaks from [[9]]): f_r = 95.2(96) for $d = 8$ mm; $f_r = 88.3(88)$ for $d = 20$ mm and $f_r = 77.0(80)$ for $d = 24$ mm.

For some cases the curvature, slope and deflection versus beam coordinate and also the wavelet coefficients were calculated. Single and double cracks with the depth $d = 24$ mm were assumed. The cases $f_n = 300$ (precritical stage) and $f_n = 800$ (postcritical stage) were considered. The results are plotted in Figs 7 to 10.

8. CONCLUSIONS

A new way for treating vibrations of cracked Euler–Bernoulli beams, based on the Haar wavelets, is proposed. For testing the method, three problems are solved and numerical results are compared with the data of other authors. The main advantages of the Haar wavelet method are its mathematical simplicity rapid convergence and good capability for treating singularities. A benefit of the proposed method is also the fact that the necessary computations can be automated to a great extent. For the most time-consuming operation – for calculating integrals of the wavelet functions – universal subprograms can be put together. For solving high-order systems of linear equations, the MATLAB matrix programs have proved to be very useful. The main shortcoming of our method is the fact that at the pre-

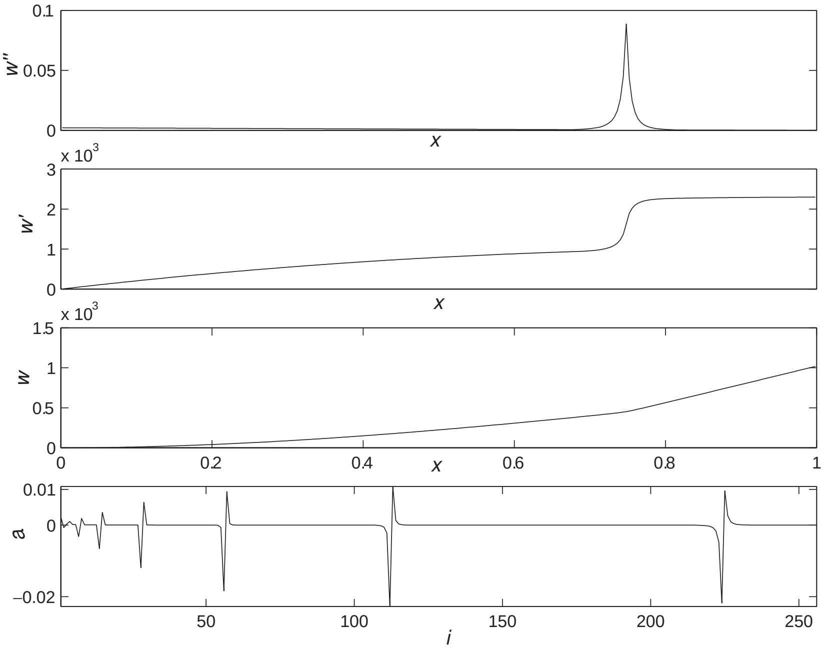

Fig. 7. Forced vibrations of the beam; single crack, precritical stage.

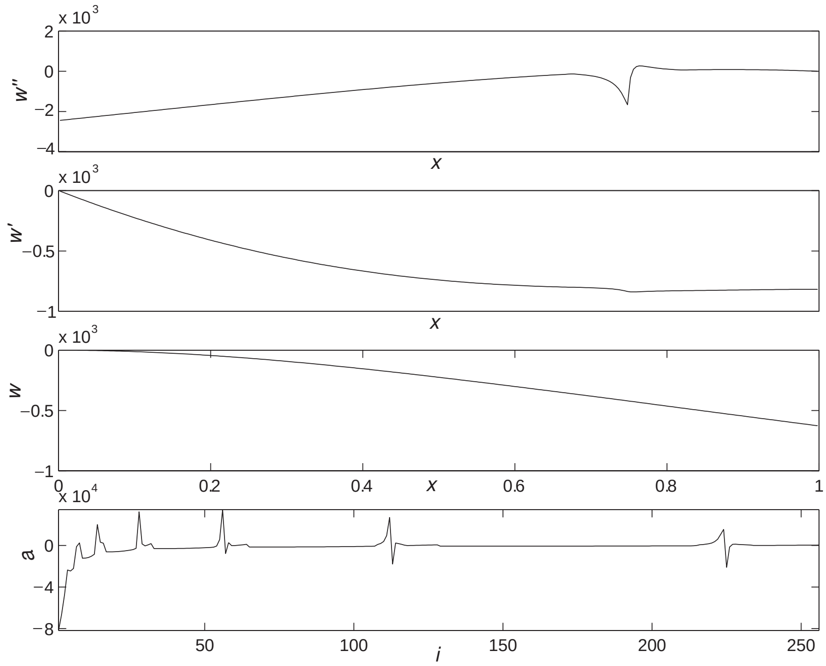

Fig. 8. Forced vibrations of the beam; single crack, postcritical stage.

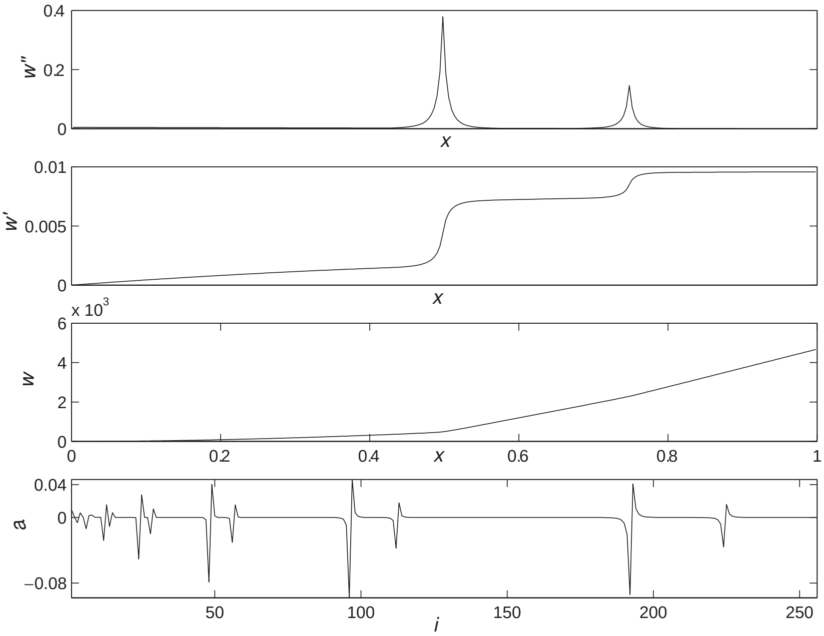

Fig. 9. Forced vibrations of the beam; two cracks, precritical stage.

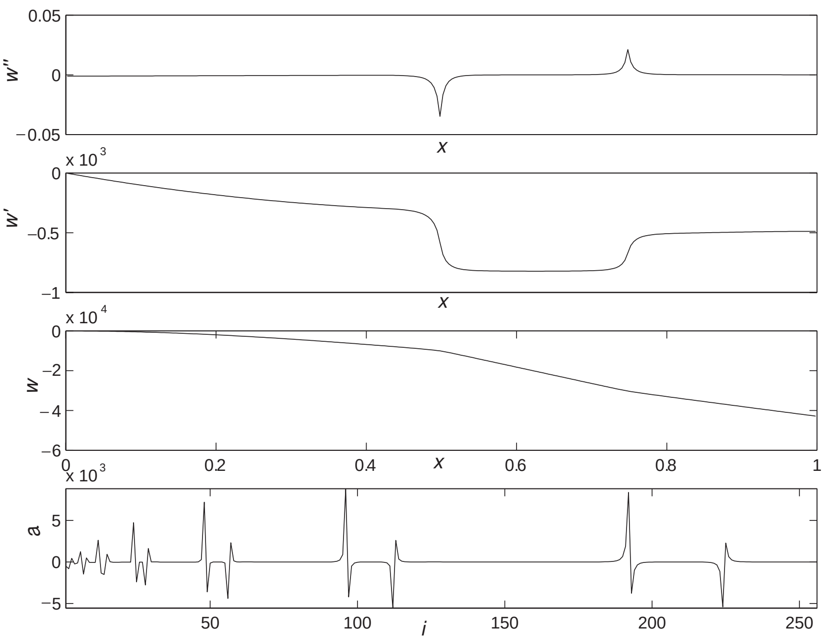

Fig. 10. Forced vibrations of the beam; two cracks, postcritical stage.

sent time we do not possess sufficiently exact methods for calculating the effective crack's width. By this reason the high accuracy of the wavelet method cannot be utilized to the full extent. In this paper only cantilever beams were considered. This is no drawback of the method – problems for other variants of boundary conditions can be treated in a similar way.

ACKNOWLEDGEMENT

Financial support of the Estonian Science Foundation (grant No. 8800) is gratefully acknowledged.

REFERENCES

1. Dimarogonas, A. D. Vibration of cracked structures: a state of the art review. *Eng. Fract. Mech.*, 1996, **55**, 831–857.
2. Doebling, S. M., Farrar, C. R. and Prime, M. B. A summary review of vibration-based damage identification methods. *Shock Vibr. Digest*, 1998, **30**, 91–105.
3. Shifrin, E. I. and Ruotolo, R. Natural frequencies of a beam with an arbitrary number of cracks. *J. Sound Vibr.*, 1999, **222**, 409–423.
4. Ruotolo, R. and Surace, C. Natural frequencies of a bar with multiple cracks. *J. Sound Vibr.*, 2004, **272**, 301–316.
5. Lin, H.-P. Direct and inverse methods on free vibration analysis of simply supported beams with a crack. *Eng. Struct.*, 2004, **26**, 427–436.
6. Wang, J. and Qiao, P. Vibration of beams with arbitrary discontinuities and boundary condition. *J. Sound Vibr.*, 2007, **308**, 12–27.
7. Lee, J. Identification of multiple cracks in a beam using vibration amplitudes. *J. Sound Vibr.*, 2009, **326**, 205–212.
8. Skrinar, M. Elastic beam finite element with an arbitrary number of transverse cracks. *Finite Element Anal. Design*, 2009, **45**, 181–189.
9. Orhan, S. Analysis of free and forced vibration of a cracked cantilever beam. *NDT E Int.*, 2007, **40**, 443–450.
10. Christides, S. and Barr, A. D. S. One dimensional theory of cracked Bernoulli–Euler beams. *Int. J. Mech. Sci.*, 1984, **26**, 639–648.
11. Sinha, J. K., Friswell, M. I. and Edwards, S. Simplified models for the location of cracks in beam structures using measured vibration data. *J. Sound Vibr.*, 2002, **251**, 13–38.
12. Carneiro, C. H. S. and Inman, D. J. Comments on the free vibrations of beams with a single edge crack. *J. Sound Vibr.*, 2001, **244**, 729–737.
13. Pugno, N. and Surace, C. Evaluation of the non-linear dynamic response to harmonic excitation of a beam with several breathing cracks. *J. Sound Vibr.*, 2009, **235**, 473–489.
14. Bovsunovski, A. P. and Matveev, V. V. Analytical approach to the determination of dynamic characteristics of a beam with a closing crack. *J. Sound Vibr.*, 2000, **235**, 415–434.
15. Chondros, T. G., Dimarogonas, A. D. and Yao, J. Vibration of a beam with a breathening crack. *J. Sound Vibr.*, 2001, **239**, 57–67.
16. Caddemi, S., Calio, I. and Marietta, M. The non-linear dynamic response of the Euler-Bernoulli beams with an arbitrary number of switching cracks. *Int. J. Non-Linear Mech.*, 2010, **45**, 714–726.
17. Biondi, B. and Caddemi, S. Closed form solutions of Euler–Bernoulli beam with singularities. *Int. J. Solids Struct.*, 2005, **42**, 3027–3044.

18. Koplow, M. A., Bhattacharyya, A. and Mann, P. M. Closed form solutions for the dynamic response of Euler–Bernoulli beams with step changes in cross-sections. *J. Sound Vibr.*, 2006, **295**, 214–225.
19. Wang, J. and Qiao, P. Vibration of beams with arbitrary discontinuities and boundary conditions. *J. Sound Vibr.*, 2007, **308**, 17–27.
20. Caddemi, S. and Calio, I. Exact closed form solution for the vibration modes of the Euler–Bernoull beam with multiple open cracks. *J. Sound Vibr.*, 2000, **327**, 749–762.
21. Caddemi, S. and Calio, I. Exact solution of the multi-cracked Euler–Bernoulli column. *Int. J. Solids Struct.*, 2008, **45**, 1332–1353.
22. Gentile, A. and Messina, A. On the continuous wavelet transforms applied to discrete vibrational data for detecting open cracks in damaged beams. *Int. J. Solids Struct.*, 2003, **40**, 295–315.
23. Zhang, W., Wang, Z. and Ma, H. Crack identification in stepped cantilever beam combining wavelet analysis with transform matrix. *Acta Mech. Solida Sinica*, 2009, **22**, 360–368.
24. Douka, E., Loutridis, S. and Trochidis, A. Crack identification in beams using wavelet analysis. *Int. J. Solids Struct.*, 2003, **40**, 3557–3569.
25. Zhong, S. and Ojadiji, S. O. Crack detection in simply supported beams without baseline modal parameters by stationary wavelet transform. *Mech. Syst. Signal Process.*, 2007, **21**, 1853–1884.
26. Quek, S.-T., Wang, Q., Zhang, L. and Ang, K. Sensitivity analysis of crack detection in beams by wavelet technique. *Int. J. Mech. Sci.*, 2001, **43**, 2899–2910.
27. Kim, B. H., Park, T. and Voyladis, G. Z. Damage estimation in beam-like structures using the multi-resolution analysis. *Int. J. Solids Struct.*, 2006, **43**, 4238–4257.
28. Lepik, Ü. Haar wavelet method for solving higher order differential equations. *Int. J. Math. Comput.*, 2008, **1**, 84–94.
29. Lepik, Ü. Numerical solution of evolution equations by the Haar wavelet method. *Appl. Math. Comput.*, 2007, **185**, 695–704.
30. Lepik, Ü. Haar wavelet method for solving stiff differential equations. *Math. Modelling and Analysis*, 2009, **10**, 1–17.
31. Cerri, M. M. and Vestroni, F. Identification of damage due to open cracks by change of measured frequencies. In *Proc. 16th IMETA Congress of Theoretical and Applied Mechanics.* Ferrari, 2003.
32. Bilello, E. *Theoretical and Experimental Investigation of Damaged Beam Under Moving System*. PhD Thesis. Universita degli Studi di Palermo. Palermo, Italy, 2001.

Praoga talade võnkumiste uurimine Haari lainikute meetodil

Ülo Lepik

Töö koosneb kahest osast. Esimeses osas on leitud täpne lahend konsooltala puhtpainde ülesandele kolme tüüpi pragude korral ja hinnatud saadud tulemusi. Teises osas on rakendatud Haari lainikute meetodit mitmete elastsete talade painde ja võnkumiste ülesannete lahendamiseks (tala paine staatilise üksikkoormuse mõjul, konsooltala vabad ning sundvõnkumised). Saadud tulemusi on võrreldud teistel meetoditel saadutega. Arvutustest nähtub, et Haari lainikute meetod kindlustab vajaliku täpsuse juba väikese arvu kollokatsioonipunktide puhul. Eriti efektiivne on soovitatud meetod singulaarsuste (praod, astmetega talad jne) korral.